Natural orbitals and their occupation numbers for free anyons in the magnetic gauge

Jerzy Cioslowski [1,2] Oliver M. Brown [3] and Tomasz Maciazek [3,*]

[1]*Institute of Physics, University of Szczecin, Wielkopolska 15, 70-451 Szczecin, Poland*

[2]*Max-Planck-Institut für Physik komplexer Systeme, Nöthnitzer Straße 38, 01187 Dresden, Germany*

[3]*School of Mathematics, University of Bristol, Fry Building, Woodland Road, Bristol BS8 1UG, United Kingdom*

(Received 26 September 2023; accepted 11 January 2024; published 9 February 2024)

We investigate the properties of natural orbitals and their occupation numbers of the ground state of two noninteracting anyons characterized by the fractional statistics parameter α and confined in a harmonic trap. We work in the boson magnetic gauge where the anyons are modeled as composite bosons with magnetic flux quanta attached to their positions. We derive an asymptotic form of the weakly occupied natural orbitals, and show that their corresponding (ordered descendingly) occupation numbers decay according to the power law $n^{-(4+2\alpha)}$, where n is the index of the natural orbital. We find remarkable numerical agreement of the theory with the natural orbitals and their occupation numbers computed from the spectral decomposition of the system's wave function. We explain that the same results apply to the fermion magnetic gauge.

DOI: 10.1103/PhysRevA.109.023316

I. INTRODUCTION

Quantum statistics describes how the wave function of a multiparticle quantum system changes under particle exchange. In three dimensions (3D), particles can have statistics that are either fermionic or bosonic. Anyons are a class of particles that exist only in two dimensions with fractional statistics, between that of bosons and fermions, allowing their states to gain arbitrary complex phases under exchange [1–5]. Such a statistic plays a role in understanding the fractional quantum Hall effect (FQHE), with emergent quasiparticles that have been identified as anyons [6]. In this model, anyons are assumed to form a noninteracting gas (reviewed in Sec. II of this paper) whose free Hamiltonian is unitarily equivalent to a system composed of either fermions or hard-core bosons with magnetic flux quanta bound to their positions [7–9]. This picture is usually refereed to as the *magnetic gauge*. The magnetic flux quanta realize the exchange phases as the Aharonov-Bohm phases. Anyons also find application in quantum computing, as the exchange of non-Abelian anyons (described by multicomponent wave functions) allows the implementation of topologically protected quantum gates which are intrinsically robust against local noise [10–13]. Such anyonic quasiparticles can be detected experimentally [14] using interferometry [15–17], correlation measurements in collider geometries [18], or spectroscopy [19].

Due to the presence of anyonic quasiparticles in the FQHE, there has recently been interest in developing the Kohn-Sham density functional theory (KS-DFT, see Refs. [20,21] for more background) for the treatment of confined noninteracting many-anyon systems. In particular, KS-DFT has been developed for anyons described as composite fluxfermions [22,23]. The reduced density matrix functional theory (RDMFT [24]) is suitable for describing strongly correlated systems [25]. As anyonic quasiparticles appear in strongly correlated systems, this method has been applied to an FQHE system [26] (specifically, to a confined quantum dot in the spin-frozen strong magnetic field regime). Recent developments in the foundations of RDMFT for bosons [27] suggest that RDMFT might be a suitable tool also for studying anyon gas in the boson magnetic gauge.

In many methods of quantum chemistry the choice of the appropriate single-particle basis is a crucial step. For instance, the Hartree-Fock method approximates the N-body wave function of a system as a single Slater determinant. This approach has been applied to study the fermion-flux composites in relation to superconductivity and the presence of the energy gap in the free anyon gas [7,28]. More generally, the multiconfigurational self-consistent field method (MCSCF) relies on superposing several Slater determinants coming from a given single-particle basis. For a given N-particle (bosonic or fermionic) quantum state, there exists a distinguished multiconfigurational expansion called the *natural expansion*. The single-particle basis that is used in the natural expansion consists of the *natural orbitals* (NOs) that are defined as eigenfunctions of the state's one-particle reduced density matrix (1RDM). It is known that natural expansion has the fastest convergence of all the possible expansions [29]. The eigenvalues of the 1RDM are called the *natural occupation numbers* (NONs) and are denoted by ν_n, $n = 1, 2, \ldots$, where $\nu_1 \geqslant \nu_2 \geqslant \cdots$. In this paper, we employ the convention for the 1RDM to be always of trace one. Due to normalization, the NONs (ordered descendingly) have to decay to zero if the single-particle basis is of infinite dimension. The rate of their

*tomasz.maciazek@bristol.ac.uk

decay reflects certain fundamental features of the system at hand. For instance, only the first N NONs of an uncorrelated state of N electrons (a Slater determinant) are nonzero. On the other hand, a slow decay of NONs characterizes a highly correlated quantum state. Furthermore, the knowledge of the NOs and NONs allows one to compute the expectation value of any one-particle observable where the individual contributions of the NOs are proportional to their corresponding NONs. For these fundamental reasons, the asymptotic rate of decay of NONs in different quantum systems has been an object of notable interest in quantum chemistry.

One of the early results in this area is Hill's asymptotic [30], which concerns ground states of two-electron systems confined in an external potential with spherical symmetry. Due to this symmetry, the 1RDM has a block-diagonal structure where the blocks are labeled by the angular momentum quantum number l. Hill's asymptotic states that the total occupancies of the blocks, $\omega_l = \sum_n \nu_{nl}$, satisfy

$$\lim_{l\to\infty} \left(l + \frac{1}{2}\right)^7 \omega_l = \mathcal{C}_H, \tag{1}$$

where $\mathcal{C}_H$ is a constant that can be computed explicitly from the given quantum state. This asymptotic behavior of ω_l was anticipated by the preceding numerical calculations for the helium atom [31,32]. Numerical calculations for the harmonium atom [33,34] further confirmed the validity of Hill's asymptotic beyond Coulomb external potentials. The large-n asymptotic of ν_{nl} (for fixed l sector) has proved to be a more difficult problem to study due to the lack of sufficiently accurate electronic structure data. Various conjectural forms of this asymptotic have been proposed and subsequently refuted over the years [32,35,36]. Finally, its correct form has been determined for ground states of two-electron systems in central potentials and proved rigorously to be [37]

$$\lim_{n\to\infty} n^8 \nu_{nl} = \mathcal{A}, \tag{2}$$

where the constant $\mathcal{A}$ does not depend on l and can be calculated explicitly from the wave function at hand. This result has been subsequently generalized to singlet states of systems with arbitrary symmetries and numbers of electrons [38]. Another work concerning general quantum systems of N Coulomb-interacting particles proved the asymptotic [39]

$$\lim_{n\to\infty} n^{\frac{8}{3}} \nu_n = \mathcal{B}, \tag{3}$$

where the constant $\mathcal{B}$ can also be calculated explicitly from the wave function [38,39]. Note the lack of the subscript l in the formula (3) that does not assume any symmetries. The above results have subsequently led to the recent discovery of a universal power law governing the accuracy of wave-function-based electronic structure calculations [40]. Similar results have been recently obtained for a system with Fermi-Huang interparticle interaction [41].

For the reliable application of quantum chemistry methods to anyonic systems, it is necessary to understand similar asymptotic behavior for models of noninteracting anyons. Here, it is relevant that anyonic systems are two-dimensional (2D), as opposed to the previously mentioned quantum-chemical systems, which are three-dimensional. Due to this change in dimensionality, new technical tools have to be applied in order to extend the methodology of the above cited papers to anyonic systems. However, the core feature remains true: the NOs and NONs are solutions to the eigenproblem of an integral operator whose kernel has a particle-particle coalescence cusp that drives the large-n asymptotic of the NOs and NONs. More specifically, as we explain in Sec. II, the coalescence cusp is proportional to $|z_1 - z_2|^\alpha$, where z_1, z_2 are the positions of the two boson-flux composite particles (represented by complex numbers) and $\alpha \in [0, 1]$ is the fractional statistics parameter. In consequence, we show that the *natural amplitudes* (NAs, the positive square roots of the NONs, $\sigma_{nl}^2 = \nu_{nl}$) of the ground state of the system at hand satisfy

$$\lim_{n\to\infty} n^{\alpha+2} \sigma_{nl} = \mathcal{D}(\alpha) \tag{4}$$

and provide explicit expression for the constant $\mathcal{D}(\alpha)$ in Eq. (37) in Sec. III. We also find very accurate asymptotic forms of the weakly occupied NOs in terms of appropriately transformed integer Bessel functions.

II. THEORETICAL BACKGROUND

Anyons have quantum statistics between fermions and bosons—the exchange of a pair of Abelian anyons results in the multiplication of the many-anyon wave function by the phase factor $e^{i\pi\alpha}$, where $\alpha \in [0, 1]$. Consequently, the wave function Ψ_α of N Abelian anyons can be expressed in terms of a bosonic wave function Ψ_B as

$$\Psi_\alpha(z_1, \ldots, z_N) = \prod_{j<k}^{N} \frac{(z_j - z_k)^\alpha}{|z_j - z_k|^\alpha} \Psi_B(z_1, \ldots, z_N), \tag{5}$$

where the complex number $z_j = x_j + iy_j$ describes the position of the jth particle, and α is the fractional statistics parameter (see, e.g., Refs. [7,42]). Similar mapping defines anyons in one dimension, where the one-body reduced density matrix of anyons confined in a harmonic trap and its NOs can be computed efficiently even for large particle numbers [43], showing that the largest NON follows a power law $\nu_1 \sim N^{p(\alpha)}$ with $0 < p(\alpha) < 1$. The anyonic wave function Ψ_α interpolates between bosons for $\alpha = 0$ and fermions for $\alpha = 1$. The free-particle Hamiltonian $\hat{H}_{\text{free}} = \nabla_1^2 + \nabla_2^2$ acting on Ψ_α then transforms under the gauge transformation in Eq. (5) to a magnetic Hamiltonian acting on Ψ_B [2,28]. In the case of two particles, this magnetic Hamiltonian in center of mass coordinates can be expressed as [44]

$$\hat{H}_B = -\frac{\hbar^2}{4m}\nabla_Z^2 + \frac{1}{m}[-i\hbar\nabla_z - e\mathbf{A}(z)]^2, \tag{6}$$

where Z is the center of mass, $z = z_1 - z_2$ is the relative coordinate, and $\mathbf{A}(z)$ is the magnetic vector potential

$$\mathbf{A}(z) = \Phi \begin{pmatrix} -\text{Im}(z_1 - z_2) \\ \text{Re}(z_1 - z_2) \end{pmatrix} = \Phi |z_1 - z_2| \hat{\mathbf{e}}_\theta, \tag{7}$$

where $e\Phi = \alpha\hbar$. In this model, the anyonic exchange phases can be thought of as Aharonov-Bohm phases due to the presence of a magnetic vector potential in the relative Hamiltonian. The bosonic Hamiltonian therefore describes boson-flux composites with hard cores.

The eigenstates for this two-anyon system in a harmonic potential are known [44]. Under the potential $V_{\text{external}} = (z_1^2 + z_2^2)/2$ (here and in the following, atomic units are used in which the harmonic potential strength, the particle mass, and $\hbar$ are all equal to one) the ground state wave function in the boson-flux composite picture is given by

$$\Psi_B^{(\alpha)}(z_1, z_2) = \mathcal{N}_\alpha \, |z_1 - z_2|^\alpha e^{-\frac{|z_1|^2+|z_2|^2}{2}},$$
$$\mathcal{N}_\alpha = \frac{1}{\pi} \frac{1}{\sqrt{2^\alpha \Gamma(\alpha+1)}}. \tag{8}$$

The NONs ν_n for a many-particle quantum system are defined as the eigenvalues of the 1RDM. Recall that for a two-particle wave function in $\mathbb{R}^d$ the 1RDM reads [45]

$$\gamma(\mathbf{r}, \mathbf{r}') = \int_{\mathbb{R}^d} d\mathbf{r}_2 \Psi(\mathbf{r}, \mathbf{r}_2) \overline{\Psi}(\mathbf{r}', \mathbf{r}_2), \tag{9}$$

and the natural orbitals ϕ_n are its eigenstates, i.e.,

$$\int_{\mathbb{R}^d} d\mathbf{r}' \gamma(\mathbf{r}, \mathbf{r}') \phi_n(\mathbf{r}') = \nu_n \phi_n(\mathbf{r}). \tag{10}$$

If the wave function Ψ is real and symmetric, it is known that its NOs and NONs can also be found by solving the following homogeneous Fredholm equation of the second kind [46], which circumvents the necessity of computing γ:

$$\int_{\mathbb{R}^d} d\mathbf{r}_2 \Psi(\mathbf{r}, \mathbf{r}_2) \phi_n(\mathbf{r}_2) = \sigma_n \phi_n(\mathbf{r_1}). \tag{11}$$

In the above equation the eigenvalues $\{\sigma_n\}_{n=1}^\infty$ are the natural amplitudes (NAs), $\nu_n = \sigma_n^2$.

Moreover, if the wave function Ψ is rotationally symmetric [as is the case for any eigenfunction of the Hamiltonian (6)], then the relevant eigenproblem is block diagonal where the blocks are enumerated by the angular momentum quantum number l. In summary, the rest of this paper will be devoted to asymptotically solving the integral equation

$$\int_{\mathbb{R}^2} dz_2 \Psi_B^{(\alpha)}(z_1, z_2) \phi_{nl}(z_2) = \sigma_{nl} \phi_{nl}(z_1), \tag{12}$$

where $\Psi_B^{(\alpha)}$ is given by formula (8), for an arbitrary fixed spin sector l, in the limit of $n \to \infty$, which means studying the weakly occupied NOs and their corresponding NAs. The key intuitions here are that (1) the radial part of ϕ_{nl} is highly oscillatory [as shown in Figs. 4(a)–4(c)—the nth numerically computed NO has $n-1$ nodes], and (2) when integrating a highly oscillatory function against a function that has discontinuous derivatives, the result goes to zero as a polynomial of the inverse of the oscillation frequency.

III. DERIVATION OF ASYMPTOTICS

Restricting to a fixed-l sector means taking the NOs of the following forms:

$$\phi_{nl}(z) = e^{i\theta l} \psi_{nl}(r) e^{-r^2/2}, \tag{13}$$

where the factor $e^{-r^2/2}$ is included for the sake of convenience. The orthonormality condition of the NOs then reads

$$2\pi \int_0^\infty r dr \, \psi_{n_1 l}(r) \psi_{n_2 l}(r) e^{-r^2} = \delta_{n_1, n_2}. \tag{14}$$

Using the relative angle variable $\theta_{12} = \theta_1 - \theta_2$ and the polar coordinates $z_j = r_j e^{i\theta_j}$, $j = 1, 2$, the Fredholm Eq. (12) becomes

$$\mathcal{N}_\alpha \int_0^\infty r_2 dr_2 \int_0^{2\pi} d\theta_{12} \cos(\theta_{12} l) \times \left(r_1^2 + r_2^2 - 2 r_1 r_2 \cos\theta_{12}\right)^{\alpha/2} e^{-r_2^2} \psi_{nl}(r_2) = \sigma_n \, \psi_{nl}(r_1). \tag{15}$$

In order to evaluate the angular integral above, note that the function $\cos(\theta_{12} l)$ can be written as a polynomial of degree $2l$ in the variable $t = [r_1^2 + r_2^2 - 2 r_1 r_2 \cos(\theta_{12})]^{1/2}$. This is because

$$\cos(\theta_{12} l) = T_l(\cos\theta_{12}) = T_l\left(\frac{r_1^2 + r_2^2 - t^2}{2 r_1 r_2}\right), \tag{16}$$

where T_l is the Chebyshev polynomial of order l, which then allows the finite polynomial expansion

$$\cos(\theta_{12} l) = \sum_{p=0}^{2l} a_p^{(l)}(r_1, r_2) t^{2p},$$

where the coefficients $a_p^{(l)}$ can be found using the explicit expansion formulas for T_l. In particular,

$$a_0^{(l)}(r_1, r_2) = T_l\left(\frac{r_1^2 + r_2^2}{2 r_1 r_2}\right).$$

Plugging this expansion into the left-hand side of (15), we get

$$\mathcal{N}_\alpha \sum_{p=0}^{2l} \int_0^\infty r_2 dr_2 \, a_p^{(l)}(r_1, r_2) e^{-r_2^2} \psi_{nl}(r_2) \times \int_0^{2\pi} d\theta_{12} \left(r_1^2 + r_2^2 - 2 r_1 r_2 \cos\theta_{12}\right)^{\alpha/2 + p} = \sigma_{nl} \, \psi_{nl}(r_1). \tag{17}$$

Next, we use the result that for any $\beta \in \mathbb{R}$,

$$\int_0^{2\pi} d\theta_{12} \left(r_1^2 + r_2^2 - 2 r_1 r_2 \cos\theta_{12}\right)^{\frac{\beta}{2}} = \pi \, G_\beta(r_1, r_2), \tag{18}$$

where

$$G_\beta(r_1, r_2) = |r_1 - r_2|^\beta \, {}_2F_1\left(\frac{1}{2}, -\frac{\beta}{2}; 1; \frac{-4 r_1 r_2}{(r_1 - r_2)^2}\right) + (r_1 + r_2)^\beta \, {}_2F_1\left(\frac{1}{2}, -\frac{\beta}{2}; 1; \frac{4 r_1 r_2}{(r_1 + r_2)^2}\right), \tag{19}$$

and ${}_2F_1$ is the ordinary hypergeometric function.

So far, all the calculations have been exact. However, we will next start making approximations in order to make the large-n asymptotic solution to Eq. (15) more tractable. The key fact to notice is that the leading contribution to the $n \to \infty$ asymptotic of σ_n comes from the lowest-order cusp of the left-hand side of Eq. (15) around $r_1 = r_2$. Let us next look at the asymptotic expansion of $G_\beta(r_1, r_2)$ around $r_1 = r_2$ when $0 < \beta < 1$. The only contribution to the cusp around $r_1 = r_2$ is the first term in the right-hand side of Eq. (19). Its

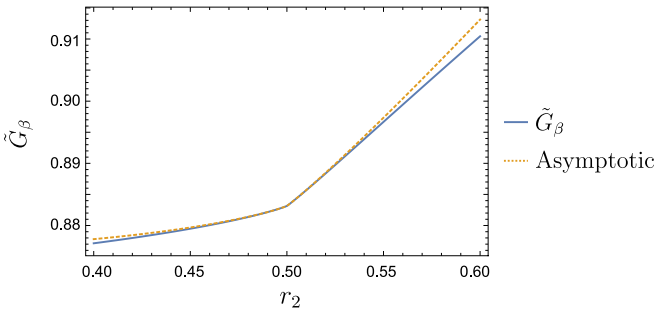

FIG. 1. The leading-order cusp in the function $\tilde{G}_\beta(r_1, r_2)$ is reproduced by the first three terms of its asymptotic expansion around $r_1 = r_2$. The plot shows the function $\tilde{G}_\beta(r_1, r_2)$ vs the first three terms of its leading-order asymptotic expansion (20) for $\beta = 1/5$, $r_1 = 0.5$.

asymptotic expansion reads

$$\begin{aligned}\tilde{G}_\beta(r_1, r_2) &= |r_1 - r_2|^\beta \, {}_2F_1\left(\frac{1}{2}, -\frac{\beta}{2}; 1; \frac{-4r_1r_2}{(r_1 - r_2)^2}\right) \\ &= \frac{2^\beta \, \Gamma\left(\frac{1+\beta}{2}\right)}{\sqrt{\pi}\Gamma\left(1 + \frac{\beta}{2}\right)} r_1^\beta - \frac{\beta \, 2^{\beta-1} \, \Gamma\left(\frac{1+\beta}{2}\right)}{\sqrt{\pi} \, \Gamma(1 + \frac{\beta}{2})} r_1^{\beta-1} \\ &\quad \times (r_1 - r_2) + \frac{\Gamma\left(-\frac{1+\beta}{2}\right)}{2\sqrt{\pi} \, \Gamma\left(-\frac{\beta}{2}\right)} \frac{1}{r_1} |r_1 - r_2|^{\beta+1} \\ &\quad + O((r_1 - r_2)^2). \end{aligned} \tag{20}$$

The first three terms of this expansion are plotted in Fig. 1. In the above formula, we can see that the leading-order cusp is $|r_1 - r_2|^{\beta+1}$. Similarly, when $\beta > 1$ the analogous cusp will appear in the order $\beta + 1$. This in turn means that the leading-order cusp in Eq. (17) will come from the $(p = 0)$-summand. Thus, the large-n asymptotic solution to Eq. (15) can be obtained from the following equation, which extracts only the leading-order cusp around $r_1 = r_2$:

$$\begin{aligned}&\mathcal{B}(\alpha) \int_0^\infty r_2 dr_2 \, |r_1 - r_2|^{\alpha+1} e^{-r_2^2} \, \psi_{nl}(r_2) \\ &= \sigma_{nl} \, r_1 \psi_{nl}(r_1), \\ &\mathcal{B}(\alpha) = \sqrt{\frac{1}{2^\alpha \, \pi \, \Gamma(\alpha + 1)}} \frac{\Gamma\left(-\frac{1+\alpha}{2}\right)}{2 \, \Gamma\left(-\frac{\alpha}{2}\right)}. \end{aligned} \tag{21}$$

In the above equation we have also used the fact that $a_0^{(l)}(r_1, r_1) = 1$.

In analogy to the three-dimensional case [37], we choose an ansatz for $\psi_{n,l}$ of the form

$$\psi_{nl}(r) = f_{nl}(r) \, J_l(\kappa_{nl} g_{nl}(r)), \tag{22}$$

where

$$\begin{aligned}&f_{nl}(r), \; g_{nl}(r) > 0, \quad g'_{nl}(r) > 0, \quad \kappa_{nl} > 0, \\ &\infty > \lim_{r\to 0} f_{nl}(r) > 0, \quad \infty > \lim_{r\to 0} \frac{g_{nl}(r)}{r} > 0. \end{aligned}$$

Functions J_l are the Bessel functions of the first kind. As previously mentioned, taking the limit $n \to \infty$ means considering highly oscillatory NOs, thus we necessarily have $\kappa_{nl} \gg 1$. The strategy is now to extract the leading order expansion of Eq. (21) in the powers of $1/\kappa_{nl}$, which will lead us to certain consistency condition for the function $g_{nl}(r)$. Because κ_{nl} is large, we can approximate the Bessel functions as [47]

$$J_l(z) \approx \sqrt{\frac{2}{\pi z}} \cos\left[z - (2l + 1)\frac{\pi}{4}\right]. \tag{23}$$

For convenience, we will ignore the phase shift proportional to $\pi/4$ under the cosine, as it will not alter the resulting consistency relations. Consequently, the integral equation (21) becomes

$$\begin{aligned}&\mathcal{B}(\alpha) \int_0^\infty dr_2 \, |r_1 - r_2|^{\alpha+1} \, \frac{r_2 \, e^{-r_2^2} f_{nl}(r_2)}{\sqrt{g_{nl}(r_2)}} \cos(\kappa_{nl} g_{nl}(r_2)) \\ &= \sigma_{nl} \, r_1 \, \frac{f_{nl}(r_1)}{\sqrt{g_{nl}(r_1)}} \cos(\kappa_{nl} g_{nl}(r_1)). \end{aligned} \tag{24}$$

With the change of variables $u_i := g_{nl}(r_i) \quad i = 1, 2$, $q(u) := g_{nl}^{-1}(u)$, we define

$$F(u_2) = \frac{1}{\sqrt{u_2}} q(u_2) \, q'(u_2) \, e^{-(q(u_2))^2} f_{nl}(q(u_2)).$$

Next, we extract the leading asymptotic around $u_1 = u_2$ using the fact that

$$\begin{aligned}|q(u_1) - q(u_2)|^{\alpha+1} &= |u_1 - u_2|^{\alpha+1} [q'(u_1)]^{\alpha+1} \\ &\quad + O(|u_1 - u_2|^{\alpha+2}). \end{aligned}$$

This allows us to write the integral Eq. (24) as

$$\begin{aligned}&\mathcal{B}(\alpha) \, \mathrm{Re}\left\{\int_0^{u_\infty} du_2 \, F(u_2) |u_1 - u_2|^{\alpha+1} e^{i\kappa_{nl} u_2}\right\} \\ &= \sigma_{nl} \, \frac{q(u_1) f_{nl}(q(u_1))}{\sqrt{u_1}(q'(u_1))^{\alpha+1}} \cos(\kappa_{nl} u_1), \end{aligned} \tag{25}$$

where $u_\infty = \lim_{r\to\infty} g_{nl}(r)$. Finally, we use a theorem from the paper [48] to extract the leading order behavior when in $\kappa_{nl} \to \infty$ (see the Appendix for more details). This leads to

$$\begin{aligned}&-\frac{2}{\kappa_{nl}^{\alpha+2}} \cos\left(\frac{\pi\alpha}{2}\right) \cos(\kappa_{nl} u_1) F(u_1) \Gamma(\alpha + 2) \\ &= \sigma_{nl} \, q(u_1) \, \frac{q(u_1) f_{nl}(q(u_1))}{\mathcal{B}(\alpha)\sqrt{u_1}(q'(u_1))^{\alpha+1}} \cos(\kappa_{nl} u_1). \end{aligned} \tag{26}$$

Equating coefficients of $\cos(\kappa_{nl} u_1)$ and expressing everything back in terms of the variable r, we arrive at the following consistency condition defining $g_{nl}(r)$:

$$\begin{aligned}\kappa_{nl} \, g_{nl}(r) &= \left(-\frac{\mathcal{C}(\alpha)}{\sigma_{nl}}\right)^{\frac{1}{\alpha+2}} \int_0^r dr_1 \, e^{-r_1^2/(\alpha+2)} \\ &= \left(-\frac{\mathcal{C}(\alpha)}{\sigma_{nl}}\right)^{\frac{1}{\alpha+2}} \mathcal{I}_\infty(\alpha) \mathrm{erf}\left(\frac{r}{\sqrt{\alpha + 2}}\right), \end{aligned} \tag{27}$$

where erf is the error function,

$$\mathcal{I}_\infty(\alpha) = \int_0^\infty dr_1 \, e^{-r_1^2/(\alpha+2)} = \frac{\sqrt{\pi(\alpha + 2)}}{2}, \tag{28}$$

and

$$\mathcal{C}(\alpha) = 2\mathcal{B}(\alpha)\Gamma(\alpha + 2) \cos\left(\frac{\pi\alpha}{2}\right). \tag{29}$$

In order to determine the dependence of σ_{nl} and κ_{nl} on n together with the form of the function f_{nl}, we refer to the

orthonormality condition of the NOs (14), which takes the explicit form

$$2\pi \int_0^\infty r dr f_{n_1 l}(r) f_{n_2 l}(r) J_l(\kappa_{n_1} g_{n_1 l}(r)) J_l(\kappa_{n_2} g_{n_2 l}(r)) e^{-r^2} = \delta_{n_1,n_2}. \tag{30}$$

In order to satisfy the above equality, we will make use of the orthogonality relation for Bessel functions [47]

$$\int_0^1 dz\, J_l(\mu_{n_1} z) J_l(\mu_{n_2} z) z = \frac{1}{2} J_l'(\mu_{n_1})^2\, \delta_{n_1,n_2}, \tag{31}$$

where μ_n is the nth node of J_l. Note first that if we require the relation

$$\sqrt{\frac{r e^{-r^2}}{g_{nl}(r)\, g_{nl}'(r)}} f_{nl}(r) \equiv \mathcal{C}_{nl} \tag{32}$$

to be satisfied and require that $g_{n_1 l}(r) = g_{n_2 l}(r) \equiv g_l(r)$, we can readily apply the identity (31) to the left-hand side of (30) after the familiar change of variables $u = g_l(r)$ under the integral. Additionally, recall that the nth NO must have $n-1$ nodes. In light of Eq. (27), this requires identifying the functions $g_{nl}(r)$ and κ_{nl} as

$$g_{nl}(r) \equiv g(r) = \mathrm{erf}\left(\frac{r}{\sqrt{\alpha+2}}\right), \quad \kappa_{nl} = \mu_n. \tag{33}$$

Consequently, we get that

$$\left(-\frac{\mathcal{C}(\alpha)}{\sigma_{nl}}\right)^{\frac{1}{\alpha+2}} \mathcal{I}_\infty(\alpha) = \mu_n. \tag{34}$$

From the relation (32) we determine that $f_{nl}(r)$ takes the form

$$f_{nl}(r) = \mathcal{C}_{nl} \sqrt{\frac{\mathrm{erf}\frac{r}{\sqrt{\alpha+2}}}{r}} e^{-\frac{r^2}{2(\alpha+2)}} e^{\frac{r^2}{2}}, \tag{35}$$

where the normalization factor reads

$$\mathcal{C}_{nl} = \frac{1}{|J_l'(\mu_n)|} \sqrt{\frac{2}{\pi\sqrt{\pi}(\alpha+2)}}. \tag{36}$$

Using the well-known asymptotic for the nodes of the Bessel functions $\mu_n \approx n\pi$, we summarize the results of this section as follows:

$$\lim_{n\to\infty} |\sigma_{nl}|\, n^{\alpha+2} = \mathcal{D}(\alpha),$$
$$\mathcal{D}(\alpha) = \frac{(2\pi)^{-\alpha/2}(\alpha+2)^{\frac{\alpha}{2}+1}}{\sin\left(\frac{\pi\alpha}{2}\right)\Gamma\left(-\frac{\alpha}{2}\right)^2\sqrt{\Gamma(\alpha+1)}}. \tag{37}$$

$$\phi_{nl}(r,\theta) \xrightarrow{n\to\infty} \mathcal{C}_{nl} \sqrt{\frac{\mathrm{erf}\frac{r}{\sqrt{\alpha+2}}}{r}} e^{-\frac{r^2}{2(\alpha+2)}} \times J_l\left[\mu_n \mathrm{erf}\left(\frac{r}{\sqrt{\alpha+2}}\right)\right] e^{i\theta l}. \tag{38}$$

IV. NUMERICAL METHODS

In this section, we carry out the numerical verification of the asymptotics predicted in Eqs. (37) and (38). This is done by writing Eq. (12) in the (κ-scaled) harmonic oscillator eigenbasis

$$\tilde{\phi}_{ml}^{(\kappa)}(r,\theta) = \mathcal{N}_{ml}^{(\kappa)} e^{i\theta l} (\kappa r)^{|l|} L_m^{|l|}(\kappa^2 r^2) e^{-\kappa^2 r^2/2},$$
$$\mathcal{N}_{ml}^{(\kappa)} = \kappa \sqrt{\frac{m!}{\pi (m+|l|)!}}, \tag{39}$$

where $\kappa > 0$ and $L_m^{|l|}$ is a generalized Laguerre polynomial. These calculations are specific to $l = 0$. As will be explained later, the parameter κ will be optimized, which allows us to pick the basis in which the NONs converge at the fastest rate. To simplify the notation we omit the l subscripts, i.e., we write $\tilde{\phi}_{m,0}^{(\kappa)} \equiv \tilde{\phi}_m^{(\kappa)}$.

In the truncated basis $\phi_m^{(\kappa)}$, $m = 0, 1, \ldots, M$, Eq. (12) for $l = 0$ is solved via the diagonalization of the $(M+1)\times(M+1)$ matrix

$$[A^{(\alpha)}(\kappa)]_{m_1,m_2} = \left\langle \phi_{m_1}^{(\kappa)}(z_1)\phi_{m_2}^{(\kappa)}(z_2) \,\middle|\, \Psi_B^{(\alpha)}(z_1,z_2)\right\rangle. \tag{40}$$

Let us next briefly describe the steps that we apply in order to evaluate some of the multidimensional integrals in the Eq. (40). Similarly to the methodology of Sec. III, we use the relative angle θ_{12} and compute the corresponding integral over θ_{12} using the result from Eq. (18). Next, we change the the radial coordinates r_1, r_2 to $r_1 = r\cos\xi$ and $r_2 = r\sin\xi$, $0 \leqslant r \leqslant \infty, \xi \in [0, \pi/2]$. The Jacobian of this transformation is r. Under this change of variables, we have

$$\pi\, G_\alpha(r\cos\xi, r\sin\xi) = r^\alpha K_\alpha(\xi), \tag{41}$$

where the function $K_\alpha(\xi)$ reads (after using an identity for the hypergeometric function to simplify its form)

$$K_\alpha(\xi) = -\frac{2\sqrt{\pi}\,\Gamma\left(\frac{2+\alpha}{2}\right)}{\Gamma\left(\frac{3+\alpha}{2}\right)} \frac{[1+\sin(2\xi)]^{\frac{2+\alpha}{2}}}{|\cos(2\xi)|} \mathrm{Im}\left\{ {}_2F_1\left[\frac{2+\alpha}{2}, \frac{1}{2}, \frac{3+\alpha}{2}, \left(\frac{1+\sin(2\xi)}{\cos(2\xi)}\right)^2\right]\right\}.$$

Next, we apply the polynomial expansions of the Laguerre polynomials. It turns out that the integrals over r can be computed analytically in terms of the Euler gamma functions. Thus, we are only left with the task of evaluating numerically the integrals over ξ. After the above transformations, the matrix elements read

$$[A^{(\alpha)}(\kappa)]_{m_1,m_2} = \frac{\mathcal{N}_\alpha}{2\kappa^{\alpha/2}} \sum_{a=0}^{m_1}\sum_{b=0}^{m_2} \binom{m_1}{a}\binom{m_2}{b} \frac{(-1)^{a+b}}{a!b!} \left(\frac{2\kappa}{\kappa^2+1}\right)^{2+a+b+\frac{\alpha}{2}} \Gamma\left(2+a+b+\frac{\alpha}{2}\right) \times \left[\sum_{j=0}^{a}(-1)^j\binom{a}{j}\mathcal{J}_{b+j}^{(\alpha)} + \sum_{j=0}^{b}(-1)^j\binom{b}{j}\mathcal{J}_{a+j}^{(\alpha)}\right], \tag{42}$$

where the integration over ξ appears only in the integrals

$$\mathcal{J}_k^{(\alpha)} = \int_0^{\pi/4} d\xi \ \sin(2\xi) K_\alpha(\xi) \cos^{2k}(\xi). \tag{43}$$

Note that in order to evaluate the expressions (42) numerically for all $0 \leqslant m_1, m_2 \leqslant M$, we only need the integrals $\mathcal{J}_k^{(\alpha)}$ for $k = 0, 1, \ldots, 2M$ which can be precalculated separately. The difficulty of this approach is that we need to know the values of the integrals $\mathcal{J}_k^{(\alpha)}$ with very high precision, because they enter the alternating sums in Eq. (42). To this end, we have used PYTHON's library MPMATH. For the calculations presented in this section, we have set the size of the one-particle basis to $M = 400$ and the precision to $2M$. Note also that the expressions (42) can be computed efficiently for all $0 \leqslant m_1, m_2 \leqslant M$ at once using the vectorisation technique, i.e., by recognizing that Eq. (42) allows one to express matrix $A^{(\alpha)}(\kappa)$ as a product of three matrices.

The optimal parameter κ has been chosen by maximizing the fidelity

$$\mathcal{F}_M^{(\alpha)}(\kappa) = \sum_{m_1,m_2=0}^{M} \left|A^{(\alpha)}_{m_1,m_2}(\kappa)\right|^2. \tag{44}$$

It has turned out that the optimal value of κ is approximately independent of α, and for $M = 400$ it is $\kappa_{\rm opt} \approx 7$.

The resulting NAs are plotted in Fig. 2. Thanks to the optimal choice of the parameter κ, we have obtained the convergence of the first 105–125 highest NAs (the exact number depends on α) with the single-particle basis of the size $M = 400$. In Fig. 2 we have plotted the values of $n^{\alpha+2}\,\sigma_n$ vs $1/n$, which allowed us to determine the values of the constants $\mathcal{D}(\alpha)$ with the relative accuracy of the order 10^{-3}. As shown in Table I and Fig. 3, this is in perfect agreement with the theoretical values calculated from Eq. (37).

In Fig. 4 we have plotted the numerically calculated NOs and compared them with their asymptotic forms from Eq. (38). We observe remarkable agreement of the asymptotic form even for values of n as low as 30. For the convenience of comparison, in the bottom row of Fig. 4 we have plotted the values of $\phi_n(r)\sqrt{r}e^{r^2/[2(\alpha+2)]}$ vs $g(r)$, which extracts the oscillatory part of the NOs. One can see that the NOs converge to their respective asymptotic forms very fast.

TABLE I. Comparison of the values of the constant $\mathcal{D}(\alpha)$ computed via the fifth-order polynomial regression in Fig. 2 for $l = 0$ with the exact formula from Eq. (37).

α	Fitted $\mathcal{D}(\alpha)$	Exact $\mathcal{D}(\alpha)$
1/5	0.0586 ± 0.0004	0.058580 . . .
2/5	0.1055 ± 0.0005	0.105525 . . .
3/5	0.1394 ± 0.0005	0.139367 . . .
4/5	0.1593 ± 0.0005	0.159293 . . .
1	0.1649 ± 0.0005	0.164961 . . .

V. CONSEQUENCES OF THE NO AND NA ASYMPTOTICS FOR COMPUTING ANYON CORRELATIONS

The asymptotic properties of NOs and NAs derived in the preceding sections are of broad relevance to physics of anyonic systems as they show universal properties of anyonic wave functions. In particular, our results show that when an anyonic wave function is expanded in a single-particle basis, the convergence of such an expansion is much slower than in the case of fermionic or bosonic systems. This has fundamental consequences for applications of any numerical methods to anyonic systems. These consequences are particularly evident in two-particle systems where the natural orbitals and natural occupation numbers allow one to reconstruct the two-anyon wave function (up to a diagonal rotation of the single-particle basis), making it possible to compute the expectation value of any quantum observable. Such two-anyon systems have been extensively studied from the point of view of anyon correlations and anyon interferometry [49–54] (including recent experimental proofs of anyonic statistics [16,18]), where one

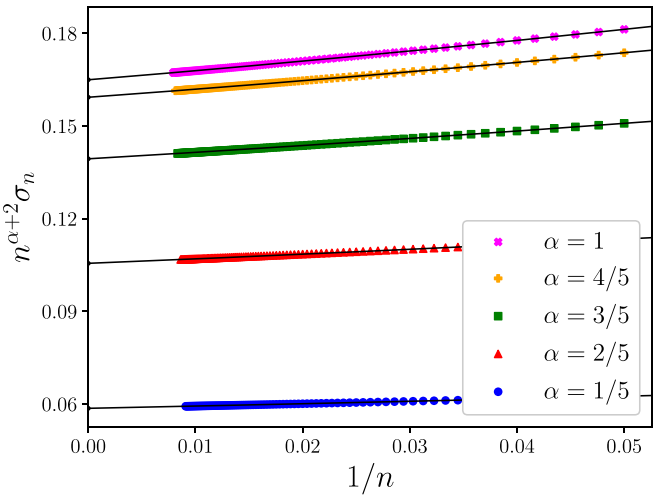

FIG. 2. NAs of the $l = 0$ sector for $\alpha \in \{\frac{1}{5}, \frac{2}{5}, \frac{3}{5}, \frac{4}{5}, 1\}$ and $M = 400$. The number n represents the index of the values σ_n. The solid lines show the outcome of the fifth-order polynomial regression for each value of α.

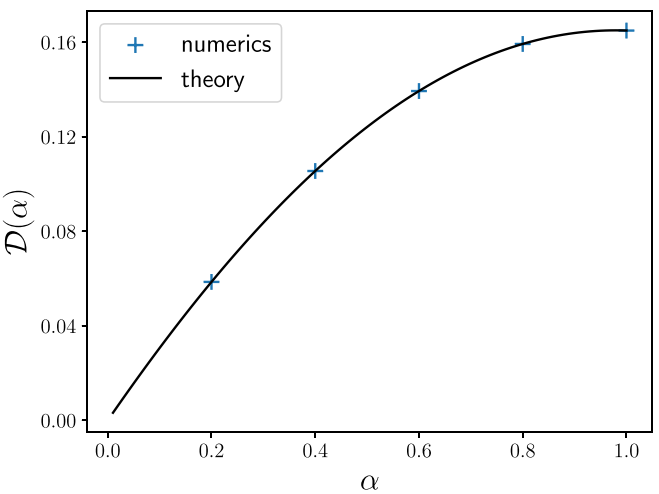

FIG. 3. The fitted values of $\mathcal{D}(\alpha)$ from fifth-order polynomial regression for $\alpha \in \{\frac{1}{5}, \frac{2}{5}, \frac{3}{5}, \frac{4}{5}, 1\}$ and $M = 400$. They are in perfect agreement with the formula (37).

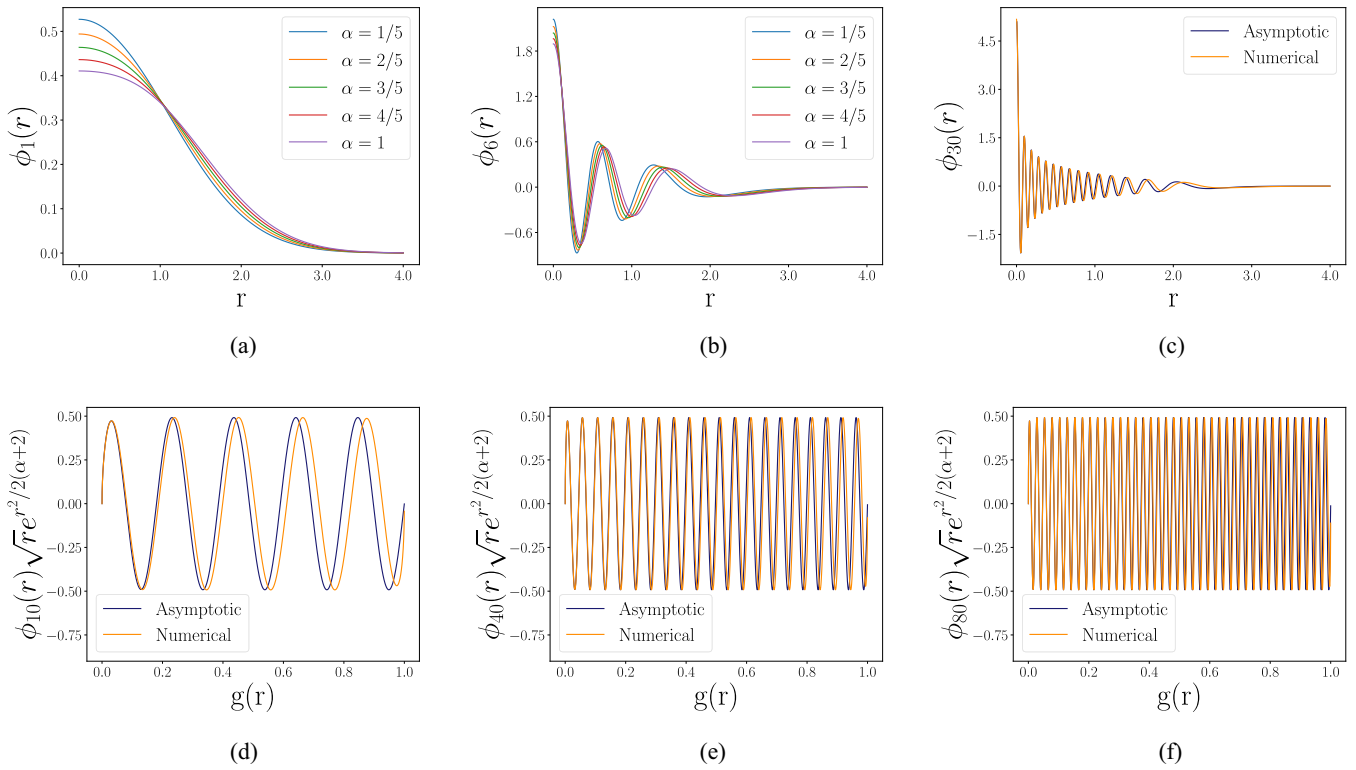

FIG. 4. Top row: the $l = 0$ natural orbitals of index 1 (a) and 6 (b) for various values of the fractional statistics parameter α. Frame (c) shows a comparison of the numerical and asymptotic forms of the natural orbital $n = 30$, for which $l = 0$ and $\alpha = 1/5$. The natural orbitals are observed to cross the axis $n - 1$ times, where n is the order of the orbital. Bottom row: a comparison of the numerically computed natural orbitals to their corresponding asymptotic formulas for large n, all with $l = 0$ and $\alpha = 1/5$. For small r the deviations negligible. Frames (d)–(f) show the oscillatory component of the natural orbitals, with $n = 10$ (d), $n = 40$ (e), and $n = 80$ (f). For small n, the deviations from the asymptotic formula diverge as r increases from 0. This divergence is less pronounced for larger n.

of the relevant observables is the two-body observable called the bunching parameter [54].

In this section, we show in detail how to calculate such expectation values using the example of two-particle correlation coefficient τ defined as

$$\tau = \frac{2\langle r_1 r_2 \cos\theta_{12}\rangle}{\langle r_1^2 + r_2^2\rangle}, \tag{45}$$

where we parametrize the configuration space of the anyons via $z_j = r_j e^{i\theta_j}$, $j = 1, 2$ with $\theta_{12} = \theta_1 - \theta_2$ being the angle between the position vectors of the anyons. The correlation coefficient τ has been originally introduced in the context of electronic wave functions [55], however it is closely related to the anyon bunching parameter introduced more recently [54].

In order to calculate the correlation coefficient τ for the two-anyon system at hand, we will work in the boson magnetic gauge, i.e., use the wave function $\Psi_B^{(\alpha)}$ defined in (8). It is convenient to change the variables to the center of mass Z and relative position z, given by

$$Z = \tfrac{1}{2}(z_1 + z_2), \quad z = z_1 - z_2. \tag{46}$$

In the new coordinates, the two-anyon wave function has the product form

$$\Psi_B^{(\alpha)}(z_1, z_2) = \mathcal{N}_\alpha e^{-|Z|^2}|z|^\alpha e^{-|z|^2/4}. \tag{47}$$

What is more, the correlation coefficient also takes a simple form in the new coordinates, i.e.,

$$\tau = \frac{4\langle|Z|^2\rangle - \langle|z|^2\rangle}{4\langle|Z|^2\rangle + \langle|z|^2\rangle}. \tag{48}$$

It is a matter of a straightforward calculation to find the relevant expectation values. The result reads

$$\tau = -\frac{\alpha}{2+\alpha}. \tag{49}$$

Recall that for $\alpha = 0$ the quantum state $\Psi_B^{(\alpha)}$ is just a product state of two bosons which is uncorrelated. Consequently, the correlation coefficient vanishes for $\alpha = 0$. What is more, τ is a monotonic function of the statistics parameter α and it reaches its minimum value $\tau = -1/3$ for $\alpha = 1$, i.e., when the wave function $\Psi_B^{(\alpha)}$ describes a strongly correlated state of two hard-core bosons.

Let us next take a closer look at how to compute the above correlation coefficient τ with the NOs of $\Psi_B^{(\alpha)}$. The two-anyon wave function can be written as

$$\Psi_B^{(\alpha)}(z_1, z_2) = \sum_{l=0}^{\infty}\sum_{n=0}^{\infty} c_{n,l}\phi_{n,l}(z_1)\phi_{n,-l}(z_2), \tag{50}$$

where $\phi_{n,l}$ are the NOs and $|c_{nl}| = |\sigma_{nl}|$ are the corresponding NAs. Then, the correlation coefficient takes the form [55]

$$\tau = \frac{\sum_{n_1,n_2,l_1,l_2} c_{n_1,l_1} c_{n_2,l_2} |\langle \phi_{n_1,l_1}| z |\phi_{n_2,l_2}\rangle|^2}{\sum_{n,l} (c_{n,l})^2 \langle \phi_{n,l}| z |\phi_{n,l}\rangle}. \tag{51}$$

Note that only those terms for which $|l_1 - l_2| = 1$ contribute to the numerator; otherwise, $\langle \phi_{n_1,l_1}| z |\phi_{n_2,l_2}\rangle$ vanishes. Although the closed forms of the expectation values in the formula (51) are difficult to find, numerics using the approximate NOs (38) show that the convergence of the expression (51) is rather slow, requiring the calculation of thousands of terms to get numerically close to the analytic value (49).

VI. DISCUSSION AND CONCLUSIONS

In this work we have analyzed the asymptotic behavior of the natural orbitals and their occupation numbers and natural amplitudes in the ground state of two noninteracting anyons in the boson magnetic gauge. We have derived exact asymptotic forms of the natural orbitals from a fixed l sector of the 1RDM when the ordinal number of the orbital n that indexes NOs and NAs tends to infinity (the latter are arranged descendingly according to their absolute values). While the asymptotic forms of NOs and NAs differ from their actual values for small n, the convergence is surprisingly fast when increasing n.

Although our calculations were done for the ground state only, the methodology can be applied *mutatis mutandis* to any other eigenstate (see Ref. [44] for their explicit forms) of this two-anyon system, resulting in the same NA asymptotic with suitably altered constant $\mathcal{D}(\alpha)$. Our asymptotic results may also extend to eigenstates of anyon gases with higher numbers of particles, however proving this would require using a different set of mathematical tools such as the ones applied in Ref. [39].

The same method can be employed to derive the NO and NA asymptotic for the noninteracting two-anyon system at hand in the fermion magnetic gauge. The fermionic counterpart of the wave function (8) is [42]

$$\Psi_F^{(\alpha)}(z_1, z_2) = \mathcal{N}_\alpha\, e^{i\theta_{12}} |z_1 - z_2|^\alpha e^{-\frac{|z_1|^2+|z_2|^2}{2}},$$

where θ_{12} is the angle between z_1 and z_2. Note that the coalescence cusp in Ψ_F is of the same order as the coalescence cusp of Ψ_B. By repeating the steps from Sec. III with Ψ_B replaced by Ψ_F, we arrive at the identical conclusion concerning the asymptotics of NOs and NAs in the fermion magnetic gauge.

It is interesting to note that according to the power law (37), the anyonic NONs in two dimensions decay slower than for Coulombic multielectron systems in 3D. This confirms the intuition that 2D anyon systems are characterized by strong correlations and, in light of Ref. [40], are likely to be more challenging to tackle by the standard quantum chemistry toolset.

One might be tempted to interpret our presented results in terms of the Pauli exclusion principle for anyons. However, note that the magnetic gauge transformation (5) from the bosonic wave function Ψ_B to the anyonic wave function Ψ_α is nonlocal, thus the NONs of Ψ_B are different from the NONs of Ψ_α. Moreover, only the NONs of Ψ_α are the ones that interpolate between fermionic case (Slater determinant for $\alpha = 1$) and the bosonic case (fully condensed state for $\alpha = 0$). Thus, for anyonic systems it is more appropriate to refer to gauge-invariant methods of measuring the Pauli exclusion principle such as the expectation value of the kinetic energy operator [56–58].

ACKNOWLEDGMENTS

The authors would like to thank Jonathan Robbins for helpful discussions. The numerical computations presented here were conducted using the University of Bristol HPC system (*BlueCrystal 4*). The research described in this publication has been funded by the National Science Center (Poland) under Grant No. 2022/47/B/ST4/00002. The support from Max-Planck-Institut für Physik komplexer Systeme (MPI PKS), Dresden, is also acknowledged by one of the authors (J.C.).

APPENDIX: THE LEADING-ORDER EXPANSION OF EQ. (25)

Reference [48] provides the following theorem: for any f being an analytic function in the region $\Omega = \{z \in \mathcal{C} : a \leqslant \mathrm{Re}(z) \leqslant b, \quad \mathrm{Im}(z) \geqslant 0\}$, we have

$$\begin{aligned}
&\int_a^b dx\,(x-a)^\alpha (b-x)^\beta f(x) e^{i\omega x} \\
&= \frac{i^{\alpha+1}}{\omega^{\alpha+1}} e^{i\omega a} \int_0^\infty dp \left(b - a - i\frac{p}{\omega}\right)^\beta f\left(a + i\frac{p}{\omega}\right) p^\alpha e^{-p} \\
&\quad - \frac{i^{\beta-1}}{(-1)^{\beta-1}\omega^{\beta+1}} e^{i\omega b} \int_0^\infty dp \left(b - a + i\frac{p}{\omega}\right)^\alpha \\
&\quad \times f\left(b + i\frac{p}{\omega}\right) p^\beta e^{-p}.
\end{aligned} \tag{A1}$$

Theorem (A1) as stated originally in Ref. [48] has a typographic error, and above we have provided its corrected version. In order to apply this theorem, we translate Eq. (25) to the form

$$\begin{aligned}
&\mathcal{I}_-(u_1) + \mathcal{I}_+(u_1) \\
&= \mathrm{Re}\left\{\int_0^{u_1} du_2\, F(u_2)\,(u_1 - u_2)^{\alpha+1} e^{i\kappa_{nl} u_2}\right\} \\
&\quad + \mathrm{Re}\left\{\int_{u_1}^{u_\infty} du_2\, F(u_2)\,(u_2 - u_1)^{\alpha+1} e^{i\kappa_{nl} u_2}\right\}.
\end{aligned} \tag{A2}$$

Applying Theorem (A1) to the $\mathcal{I}_-(u_1)$,

$$\begin{aligned}
&\int_0^{u_1} du_2\, F(u_2)(u_1 - u_2)^{\alpha+1} e^{i\kappa_{nl} u_2} \\
&= \frac{i}{\kappa_{nl}} \int_0^\infty dp \left(u_1 - i\frac{p}{\kappa_{nl}}\right)^{\alpha+1} F\left(i\frac{p}{\kappa_{nl}}\right) e^{-p} \\
&\quad - \frac{i^\alpha e^{i\kappa_{nl} u_1}}{(-1)^\alpha \kappa_{nl}{}^{\alpha+2}} \int_0^\infty dp\, F\left(u_1 + i\frac{p}{\kappa_{nl}}\right) p^{\alpha+1} e^{-p}.
\end{aligned}$$

Extracting the leading order asymptotics in $\kappa_{nl} \to \infty$ produces

$$\frac{i}{\kappa_{nl}} \int_0^\infty dp\, u_1^{\alpha+1} F(0) e^{-p} - \frac{i^\alpha e^{i\kappa_{nl}u_1}}{(-1)^\alpha {\kappa_{nl}}^{\alpha+2}} \int_0^\infty dp\, F(u_1) p^{\alpha+1} e^{-p} = \frac{i}{\kappa_{nl}} u_1^{\alpha+1} F(0) - \frac{i^\alpha e^{i\kappa_{nl}u_1}}{(-1)^\alpha {\kappa_{nl}}^{\alpha+2}} F(u_1)\Gamma(\alpha+2),$$

for which it is straightforward to see that $F(r) \to 0$ as $r \to 0$. Similarly, for the second integral we find

$$\int_{u_1}^{u_\infty} du_2\, F(u_2)(u_1 - u_2)^{\alpha+1} e^{i\kappa_{nl}u_2} = -\frac{i^\alpha}{\kappa_{nl}^{\alpha+2}} e^{i\kappa_{nl}u_1} F(u_1)\Gamma(\alpha+2),$$

where we use the fact that $F(r)$ must tend to zero as $r \to \infty$. Summing up, the integral sum (A2) can now be expressed as

$$\begin{aligned}\mathcal{I}_-(u_1) + \mathcal{I}_+(u_1) &= \mathrm{Re}\left\{-i^\alpha[(-1)^{-\alpha} + 1]\frac{e^{i\kappa_{nl}u_1}}{\kappa_{nl}^{\alpha+2}} F(u_1)\Gamma(\alpha+2)\right\} \\ &= -2\cos\left(\frac{\pi\alpha}{2}\right)\cos(\kappa_{nl}u_1)\frac{F(u_1)\Gamma(\alpha+2)}{\kappa_{nl}^{\alpha+2}}\end{aligned}$$

Using the above fact in (A2) yields Eq. (26).

[1] J. M. Leinaas and J. Myrheim, On the theory of identical particles, Nuovo Cim. B **37**, 1 (1977).

[2] F. Wilczek, Quantum mechanics of fractional-spin particles, Phys. Rev. Lett. **49**, 957 (1982).

[3] G. A. Goldin, R. Menikoff, and D. H. Sharp, Particle statistics from induced representations of a local current group, J. Math. Phys. **21**, 650 (1980).

[4] G. A. Goldin, R. Menikoff, and D. H. Sharp, Comments on "General theory for quantum statistics in two dimensions," Phys. Rev. Lett. **54**, 603 (1985).

[5] T. Hansson, J. Leinaas, and J. Myrheim, Dimensional reduction in anyon systems, Nucl. Phys. B **384**, 559 (1992).

[6] D. Arovas, J. R. Schrieffer, and F. Wilczek, Fractional statistics and the quantum Hall effect, Phys. Rev. Lett. **53**, 722 (1984).

[7] R. B. Laughlin, Superconducting ground state of noninteracting particles obeying fractional statistics, Phys. Rev. Lett. **60**, 2677 (1988).

[8] Y.-S. Wu, General theory for quantum statistics in two dimensions, Phys. Rev. Lett. **52**, 2103 (1984).

[9] D. Lundholm and N. Rougerie, Emergence of fractional statistics for tracer particles in a Laughlin liquid, Phys. Rev. Lett. **116**, 170401 (2016).

[10] C. Nayak, S. H. Simon, A. Stern, M. Freedman, and S. Das Sarma, Non-Abelian anyons and topological quantum computation, Rev. Mod. Phys. **80**, 1083 (2008).

[11] J. K. Pachos and S. H. Simon, Focus on topological quantum computation, New J. Phys. **16**, 065003 (2014).

[12] A. Y. Kitaev, Unpaired Majorana fermions in quantum wires, Phys. Usp. **44**, 131 (2001).

[13] A. Kitaev, Fault-tolerant quantum computation by anyons, Ann. Phys. **303**, 2 (2003).

[14] D. E. Feldman and B. I. Halperin, Fractional charge and fractional statistics in the quantum Hall effects, Rep. Prog. Phys. **84**, 076501 (2021).

[15] P. Bonderson, K. Shtengel, and J. Slingerland, Interferometry of non-Abelian anyons, Ann. Phys. **323**, 2709 (2008).

[16] J. Nakamura, S. Liang, G. C. Gardner, and M. J. Manfra, Direct observation of anyonic braiding statistics, Nat. Phys. **16**, 931 (2020).

[17] J. Nakamura, S. Liang, G. C. Gardner, and M. J. Manfra, Fabry-Pérot interferometry at the $\nu = 2/5$ fractional quantum Hall state, Phys. Rev. X **13**, 041012 (2023).

[18] H. Bartolomei, M. Kumar, R. Bisognin, A. Marguerite, J.-M. Berroir, E. Bocquillon, B. Plaçais, A. Cavanna, Q. Dong, U. Gennser, Y. Jin, and G. Fève, Fractional statistics in anyon collisions, Science **368**, 173 (2020).

[19] Z. Papić, R. S. K. Mong, A. Yazdani, and M. P. Zaletel, Imaging anyons with scanning tunneling microscopy, Phys. Rev. X **8**, 011037 (2018).

[20] P. Hohenberg and W. Kohn, Inhomogeneous electron gas, Phys. Rev. **136**, B864 (1964).

[21] W. Kohn and L. J. Sham, Self-consistent equations including exchange and correlation effects, Phys. Rev. **140**, A1133 (1965).

[22] Y. Hu and J. K. Jain, Kohn-Sham theory of the fractional quantum Hall effect, Phys. Rev. Lett. **123**, 176802 (2019).

[23] Y. Hu, G. Murthy, S. Rao, and J. K. Jain, Kohn-Sham density functional theory of Abelian anyons, Phys. Rev. B **103**, 035124 (2021).

[24] T. L. Gilbert, Hohenberg-Kohn theorem for nonlocal external potentials, Phys. Rev. B **12**, 2111 (1975).

[25] M. Rodríguez-Mayorga, E. Ramos-Cordoba, M. Via-Nadal, M. Piris, and E. Matito, Comprehensive benchmarking of density matrix functional approximations, Phys. Chem. Chem. Phys. **19**, 24029 (2017).

[26] E. Tölö and A. Harju, Reduced density-matrix functional theory in quantum Hall systems, Phys. Rev. B **81**, 075321 (2010).

[27] C. L. Benavides-Riveros, J. Wolff, M. A. L. Marques, and C. Schilling, Reduced density matrix functional theory for bosons, Phys. Rev. Lett. **124**, 180603 (2020).

[28] C. B. Hanna, R. B. Laughlin, and A. L. Fetter, Quantum mechanics of the fractional-statistics gas: Hartree-Fock approximation, Phys. Rev. B **40**, 8745 (1989).

[29] P.-O. Löwdin, Quantum theory of cohesive properties of solids, Adv. Phys. **5**, 1 (1956).
[30] R. N. Hill, Rates of convergence and error estimation formulas for the Rayleigh–Ritz variational method, J. Chem. Phys. **83**, 1173 (1985).
[31] W. Lakin, On singularities in eigenfunctions, J. Chem. Phys. **43**, 2954 (1965).
[32] D. P. Carroll, H. J. Silverstone, and R. M. Metzger, Piecewise polynomial configuration interaction natural orbital study of $1s^2$ helium, J. Chem. Phys. **71**, 4142 (1979).
[33] J. Cioslowski and M. Buchowiecki, Collective natural orbital occupancies of harmonium, J. Chem. Phys. **122**, 084102 (2005).
[34] J. Cioslowski, Partial-wave decomposition of the ground-state wavefunction of the two-electron harmonium atom, Theor. Chem. Acc. **134**, 113 (2015).
[35] C. F. Bunge, Electronic wave functions for atoms, Theor. Chim. Acta **16**, 126 (1970).
[36] J. Cioslowski and F. Prątnicki, Natural amplitudes of the ground state of the helium atom: Benchmark calculations and their relevance to the issue of unoccupied natural orbitals in the H_2 molecule, J. Chem. Phys. **150**, 074111 (2019).
[37] J. Cioslowski and F. Prątnicki, Universalities among natural orbitals and occupation numbers pertaining to ground states of two electrons in central potentials, J. Chem. Phys. **151**, 184107 (2019).
[38] J. Cioslowski and K. Strasburger, From Fredholm to Schrödinger via Eikonal: A new formalism for revealing unknown properties of natural orbitals, J. Chem. Theory Comput. **17**, 6918 (2021).
[39] A. V. Sobolev, Eigenvalue asymptotics for the one-particle density matrix, Duke Math. J. **171**, 3481 (2022).
[40] J. Cioslowski and K. Strasburger, A universal power law governing the accuracy of wave function-based electronic structure calculations, J. Phys. Chem. Lett. **13**, 8055 (2022).
[41] J. Cioslowski, B.-G. Englert, M.-I. Trappe, and J. H. Hue, Contactium: A strongly correlated model system, J. Chem. Phys. **158**, 184110 (2023).
[42] D. Lundholm, Properties of 2D anyon gas, in *Encyclopedia of Condensed Matter Physics (2nd Edition)*, edited by T. Chakraborty (Elsevier, New York, 2023).
[43] Y. Hao, Ground-state properties of hard-core anyons in a harmonic potential, Phys. Rev. A **93**, 063627 (2016).
[44] Y.-S. Wu, Multiparticle quantum mechanics obeying fractional statistics, Phys. Rev. Lett. **53**, 111 (1984).
[45] E. H. Lieb, Density functionals for Coulomb systems, Int. J. Quantum Chem. **24**, 243 (1983).
[46] P.-O. Löwdin and H. Shull, Natural orbitals in the quantum theory of two-electron systems, Phys. Rev. **101**, 1730 (1956).
[47] M. Abramowitz and I. Stegun, *Handbook of Mathematical Functions: With Formulas, Graphs, and Mathematical Tables*, Applied Mathematics Series (Dover Publications, New York, 1965).
[48] H. Kang and X. Shao, Fast computation of singular oscillatory Fourier transforms, Abstr. Appl. Anal. **2014**, 1 (2014).
[49] S. Vishveshwara, M. Stone, and D. Sen, Correlators and fractional statistics in the quantum Hall bulk, Phys. Rev. Lett. **99**, 190401 (2007).
[50] D. Sen, M. Stone, and S. Vishveshwara, Quasiparticle propagation in quantum Hall systems, Phys. Rev. B **77**, 115442 (2008).
[51] S. Vishveshwara and N. R. Cooper, Correlations and beam splitters for quantum Hall anyons, Phys. Rev. B **81**, 201306(R) (2010).
[52] B. I. Halperin, A. Stern, I. Neder, and B. Rosenow, Theory of the Fabry-Pérot quantum Hall interferometer, Phys. Rev. B **83**, 155440 (2011).
[53] B. Rosenow, I. P. Levkivskyi, and B. I. Halperin, Current correlations from a mesoscopic anyon collider, Phys. Rev. Lett. **116**, 156802 (2016).
[54] V. Subramanyan and S. Vishveshwara, Correlations, dynamics, and interferometry of anyons in the lowest Landau level, J. Stat. Mech.: Theory Exp. (2019) 104003.
[55] W. Kutzelnigg, G. Del Re, and G. Berthier, Correlation coefficients for electronic wave functions, Phys. Rev. **172**, 49 (1968).
[56] D. Lundholm and J. P. Solovej, Local exclusion principle for identical particles obeying intermediate and fractional statistics, Phys. Rev. A **88**, 062106 (2013).
[57] D. Lundholm and J. P. Solovej, Hardy and Lieb–Thirring inequalities for anyons, Commun. Math. Phys. **322**, 883 (2013).
[58] D. Lundholm and J. P. Solovej, Local exclusion and Lieb–Thirring inequalities for intermediate and fractional statistics, Ann. Henri Poincaré **15**, 1061 (2014).